G.A. Tung
B.D. Julius
J.M. Rogg

MRI of intracerebral hematoma: value of vasogenic edema ratio for predicting the cause

G.A. Tung (✉) · B.D. Julius · J.M. Rogg
Department of Diagnostic Imaging,
Brown Medical School
and Rhode Island Hospital,
593 Eddy Street, Providence,
Rhode Island, 02903, USA
E-mail: gtung@lifespan.org
Tel.: +1-401-4445184
Fax: +1-401-4445017

Abstract We evaluated a method for quantifying vasogenic edema (VE) on MRI to identify brain hematomas caused by neoplasms. We performed a blinded review of 68 acute and subacute hematomas caused by neoplasms (22), hypertension or presumed amyloid angiopathy (27), or vascular malformations (19). The extent of vasogenic edema was quantified on an axial T2-weighted image using the VE ratio: the maximum width of high signal surrounding a hematoma and the mean diameter of the hematoma. Hematomas caused by neoplasm were associated with more vasogenic edema (mean VE ratio 104% ± 15%; mean VE width 2.4 ± 0.7 cm) than non-neoplastic hematomas (mean VE ratio 37% ± 5%; P = 0.001). When the width of VE was equal to or more half the diameter the hematoma (VE ratio 50%), the positive predictive value for tumor was 66%; when it was equal to or more than the diameter, the positive predictive value was 71%. All six hematomas with VE ratios ≥150% were caused by neoplasm.

Keywords Intracerebral hemorrhage · Cerebral tumors · Vasogenic edema · Magnetic resonance imaging

Introduction

Spontaneous intracerebral hematoma is often attributed to systemic hypertension or amyloid angiopathy, but there are a number of other causes, such as primary brain tumor, metastasis, or vascular malformation [1]. One of the principal clinical concerns is to distinguish a tumor that has bled from a non-neoplastic hematoma. At our institution the radiologic evaluation of a patient with a cerebral hematoma that might be caused by a tumor includes CT of the chest, abdomen, and pelvis to search for a primary malignancy. Stereotactic brain biopsy may be performed if a primary brain tumor is suspected or if chest and body CT do not identify a primary tumor. If tumor is the cause for an intracerebral hematoma, the prognosis is poorer than for non-neoplastic hematomas [1, 2, 3].

CT is often performed initially to distinguish the acute presentation of ischemic stroke from that of intracerebral hemorrhage. Early investigations found that CT was useful for detecting intracerebral hematoma, but subsequent reports suggest that it may not be of similar value for revealing the cause [4]. MRI has also been performed to investigate the cause of intracerebral hematoma and one study found that MRI performed within 72 h of hospital presentation provided a specific new diagnosis in 22% of patients with intracerebral hematoma [5]. However, this study did not evaluate the usefulness of specific diagnostic signs on MRI. The complex appearance of an acute or subacute hematoma on MRI makes image interpretation more challenging [6, 7]. An alternative to early imaging is MRI after the hemorrhagic mass and edema have resolved, but this could delay diagnosis and therapy of an intracerebral hematoma with a treatable cause [8, 9].

Previous investigations have suggested that certain signs may provide clues to the cause of a brain hematoma on MRI [10, 11, 12, 13, 14, 15]. In a study of serial MRI, Atlas et al. [10] reported five discriminatory features of hemorrhagic intracranial neoplasms: irregular hemosiderin rim, nonhemorrhagic neoplastic tissue, marked signal heterogeneity, delayed evolution, and pronounced or persistent edema. However, this study relied on both acute and follow-up MRI, did not include a comparison cohort of non-neoplastic hematomas, and proposed no objective criteria for "pronounced edema". Our purpose was to evaluate the diagnostic importance of vasogenic edema (VE) as a sign of tumor presenting as intracerebral hematoma. In particular, our hypothesis is that a simple method of quantifying the relative amount of vasogenic edema surrounding an intracerebral hematoma will help to classify hematomas correctly as neoplastic or non-neoplastic.

Methods

A search of our reporting system identified contrast-enhanced MRI of the brain, that contained the terms "hematoma" or "hemorrhage" in the body or conclusion of the report. The medical records were then reviewed and only cases in which MRI had been performed within 1 week of clinical presentation were included. Another inclusion criterion was a diagnosis of cause based on a suitable reference standard: brain biopsy, serial follow-up imaging, or conventional catheter angiography. Exclusion criteria included a history of recent head trauma or brain surgery, hemorrhage primarily in the subarachnoid, subdural, or intraventricular space, and hemorrhagic infarction.

Contrast-enhanced-MRI was performed at 1.5 tesla and included axial and parasagittal T1-weighted, conventional spin-echo images before and after 0.1 mmol/kg gadopentetate dimeglumine or gadoiamide intravenously, axial fast spin-echo T2-weighted, fluid-attenuated inversion recovery, and two-dimensional, fast low-angle shot, gradient-echo T2*-weighted images. Axial, fat-saturated, fast spin-echo T2-weighted images were performed with TR 4000–5000 ms, effective TE 90–140 ms, and 5 mm slice thickness, 2 mm interslice gap, 173×230 mm field of view and matrix 154×256.

Each MRI examination was reviewed by a board-certified neuroradiologist blinded to the diagnosis. The site of the hematoma was classified as cerebral lobar, basal ganglia, or posterior cranial fossa. Hematomas were classified as acute (isointense or minimal low-signal on T1- and marked low signal on T2-weighted images) or early subacute (high signal on T1- and marked low signal on T2-weighted images).

On the axial T2-weighted image on which the hematoma was visually assessed to be largest, its mean diameter was determined by taking the average of its longest diameter and its diameter perpendicular to that (Fig. 1). In a few cases, a T2*-weighted image was used to help define the margin of the hematoma, but measurements were made on the T2-weighted image. On that same image, vasogenic edema (VE) was measured as the maximum distance from the edge of the hematoma to the peripheral margin of high signal. We defined the VE ratio as follows: VE ratio (%) = (maximum width of edema÷mean diameter of hematoma)×100. Thus, if the width of the zone of vasogenic edema is half the mean diameter of the hematoma, the VE ratio is 50%.
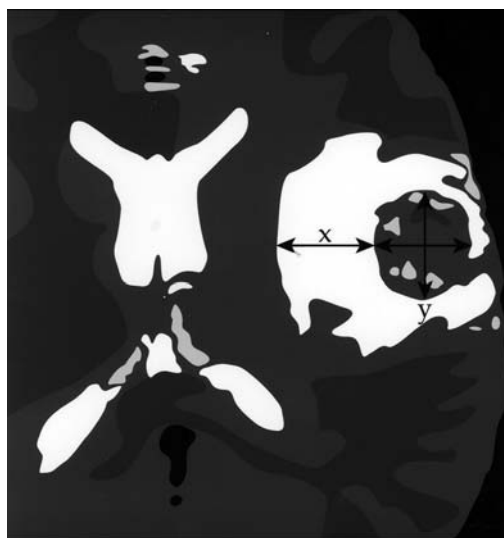

Fig. 1 Method for quantifying vasogenic edema around a hematoma. On the axial T2-weighted image in which the hematoma appears largest, its mean diameter is determined as the average of its greatest diameter and its orthogonal. Vasogenic edema is measured on the same image as the maximum distance from the edge of hematoma to the periphery of the margin of high signal around it (x). The VE ratio, expressed as a percentage, is: (maximal width of edema÷mean diameter of hematoma)x100%

The two-sided Student's t-test was used to compare the relative size and VE ratio between the different causes of hematoma. Fisher's exact test was used to compare the relative frequency distribution of hematoma site. A P value of ≤ 0.01 was taken to be statistically significant.

Results

A total of 68 enhanced-MRI examinations are the materials of this investigation, and include studies on 37 males and 31 females of mean age 51 years (range, 1–85). MRI was performed an average of 4.3 ± 1.5 days (mean $\pm$ standard deviation; range, 1 day to 7 days) after initial clinical presentation.

Based on criteria of open or stereotactic biopsy (27), serial imaging (30), and catheter angiography (10), we classified the etiology of the brain hematoma into one of three causes. The hematoma was attributed to neoplasm in 22 cases; brain biopsy was performed an average of 4.8 weeks (range 1–8 weeks) after initial MRI with pathologic diagnoses of glioblastoma multiforme (in eight cases), metastases (nine), low grade astrocytoma (three), and one case each of anaplastic astrocytoma and primitive neuroectodermal tumor. Hypertension or amyloid angiopathy (HAA) was the presumed cause in 27 cases based on follow-up CT or MRI (in 22 cases), negative angiography in three , and biopsy in two. In these cases, follow-up CT or MRI was performed on average 10.2 weeks after the initial MRI (range

1–31 weeks). The hematoma was attributed to a vascular malformation in 19 cases. A pial arteriovenous malformation was diagnosed on conventional catheter angiography (in eight cases), typically performed within 48 h of the MRI, or brain biopsy (in two). The diagnosis of cavernous hemangioma was made by brain biopsy in four cases or on follow-up MRI after resolution of the acute hematoma (in five). The diagnosis on follow-up MRI was based on the typical appearances.

We classified 27 hemorrhages (40%) as acute and 41 (60%) as early subacute. The majority (51; 73%) were in the cerebral lobes, followed by the basal ganglia (10; 16%) and posterior cranial fossa (seven; 11%). There was no significant difference ($P = 0.28$) in cause based on site since 75% of spontaneous, 61% of vascular malformation hemorrhages, and 86% of neoplasm-associated hematomas were in the cerebral lobes. The mean diameter of the hematomas was 3.2 cm for spontaneous, 3.3 cm for vascular malformation, and 3.8 cm for the neoplasm group, with no significant difference in the size between groups ($P = 0.08$).

For hematomas associated with neoplasms, the mean VE ratio was $104 \pm 15\%$ (mean ± standard error; standard deviation 69%; range 7–300%) and the average width of edema 2.4 cm ± 0.2 cm (standard deviation 0.9 cm) (Figs. 2, 3). The mean VE ratio was $26 \pm 2\%$ (standard deviation 12%; range, 5–50%) for hematomas attributed to hypertension or amyloid angiopathy, and $52 \pm 10\%$ (standard deviation 42%; range 5–140%) (Figs. 4, 5) for those with vascular malformations. Thus, for non-neoplastic hematomas (spontaneous and vascular malformation groups com-

Fig. 2a, b A 14-year-old child with coagulopathy and right inferior parietal lobar hematoma. a Axial T1-weighted spin-echo image shows a high-signal mass (*open arrow*) consistent with a subacute lobar hematoma. b On a fast spin-echo T2-weighted image, the mean diameter of the hematoma is 2.3 cm and the width of vasogenic edema (*between arrows*) is 3.2 cm; the VE ratio is 139%. Biopsy showed metastatic osteosarcoma
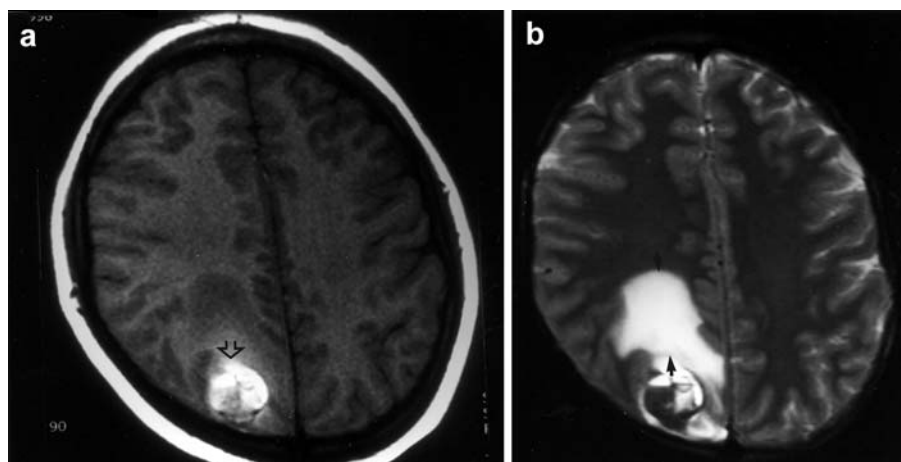

Fig. 3a, b A 6-year-old child with an acute right pontine hematoma. a CT shows dense hemorrhage (*arrow*) in the right side of the pons. b Fast spin-echo T2-weighted image 2 days later shows an enlarging hematoma (*open arrow*) that measuring 2.9 cm in average diameter. The maximum width of asymmetric high signal around it 2.9 cm (*between small white arrows*); the VE ratio is thus 100%. Biopsy revealed a glioma
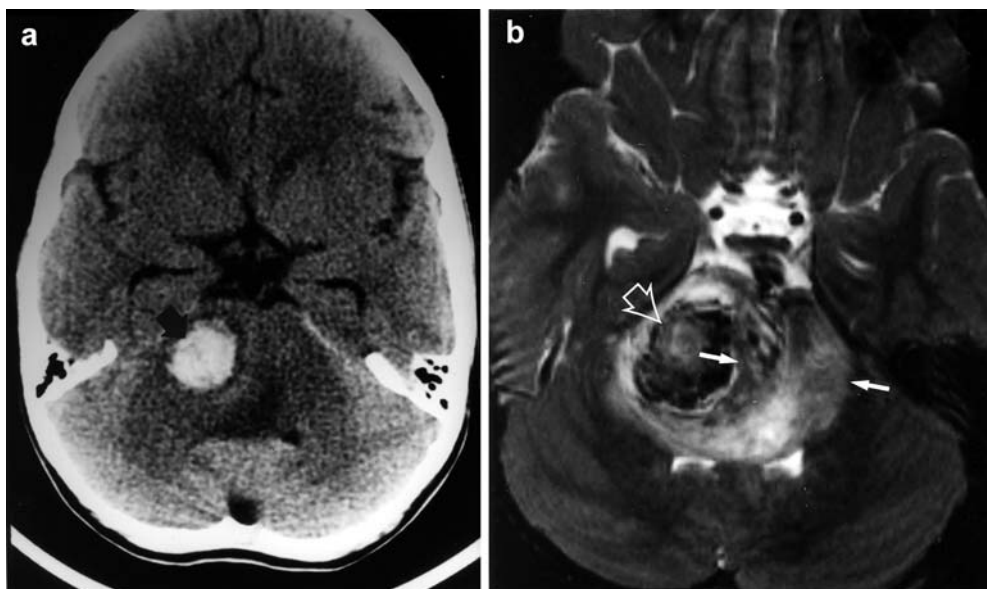
Fig. 4a, b A 7-year-old girl with an acute left temporal lobe hematoma. a Fat-saturated fast spin-echo T2-weighted image shows a hematoma, mean diameter 2.2 cm and a 0.9 cm collar of high signal; the VE ratio is 41%. b Contrast-enhanced T1-weighted image shows a focal area of enhancement (arrow) corresponding to the nidus of an arteriovenous malformation on angiography
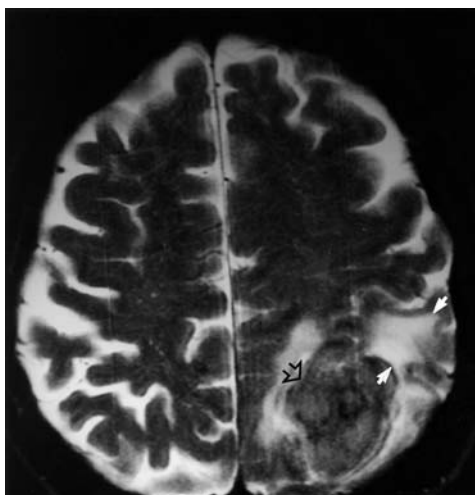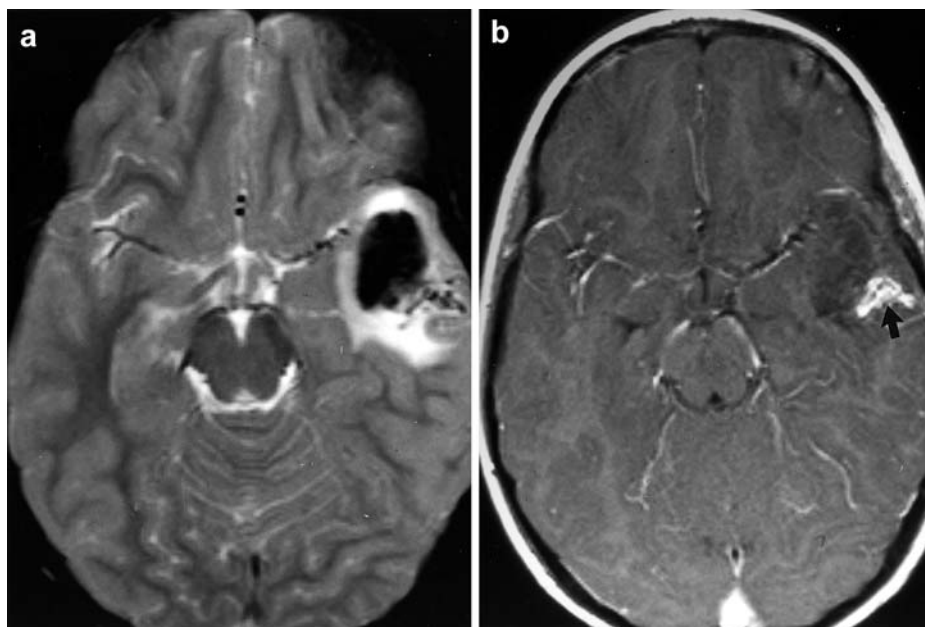

Fig. 5 A 78-year-old man with a left superior parietal hematoma. Fast spin-echo T2-weighted image shows a 3.5 cm lobar hematoma (open arrow). Maximum width of high signal around it (between small black arrows) is 1.5 cm and the VE ratio is 43%. Contrast-enhanced MRI 3 months later showed no evidence of tumor or vascular malformation

bined), the mean VE ratio was $37 \pm 5\%$ (standard deviation 31%) and average edema width was 0.9 ± 0.1 cm (standard deviation 0.5 cm). Both the VE ratio ($P = 0.009$) and the width of the zone of vasogenic edema ($P = 0.0001$) were significantly greater for neoplasm-associated hematomas.

Of the 29 hematomas with a VE ratio ≥50%, 19 (66%) were associated with a neoplasm; the sensitivity, specificity, positive and negative predictive values of this cutoff point were 86, 78, 66, and 92% respectively. Of the 14 with a ratios≥100%, that is, where the zone of edema was at least as wide as their mean diameter, 10 (71%) were associated with a tumor; the sensitivity, specificity, positive and negative predictive values were 45, 91, 71, and 78%, respectively. All six hematomas with a VE ratio≥150% were caused by neoplasm.

Discussion

The diagnosis of tumor as the underlying cause of an intracranial hematoma is both difficult and important. Although neoplasms account for only 2–10% of all brain hematomas, the prognosis is much more grave than other causes [1, 2, 3]. Significant hemorrhage is associated with up to14% of brain metastases, particularly lung carcinoma and melanoma, and with 2–4% of primary brain neoplasms, notably glioblastoma multiforme, oligodendroglioma, and ependymoma [3, 16, 17]. Our study extends the observations of Atlas et al. [10], detailed above, by suggesting a simple method for quantifying edema around a hematoma. We realize that a more accurate method of measuring the hematoma and edema would have been to trace and summate regions of interest on each image to obtain a volume. However, the VE ratio is more simple and practical. Our findings corroborate the observation of Atlas et al. [10] that tumor-associated hematomas are surrounded by a wider zone of high signal on T2-weighted images than non-neoplastic hematomas.

Although we have used the term "vasogenic edema", high signal around a tumor on T2-weighted images has been attributed to interstitial edema, microscopic infil-

trative tumor, or both. Peritumoral edema is predominantly vasogenic since "leaky" neoplastic microvessels permit extravasation of water, electrolytes, and plasma proteins into brain tissue [18, 19]. Hyperpermeability occurs because a structural deficiency of the blood brain barrier [20, 21]. The porous neovessels may also be relatively more friable and predispose to intratumoral hemorrhage [22, 23]. But in addition to a deficiency of endothelial integrity, both primary brain tumors and metastases have been shown to produce vascular endothelial permeability and growth factors [19, 21]. These cytokines act directly on endothelial cells to increase permeability selectively to proteins and are also potent mitogens that induce angiogenesis [24]. High signal around both high- and low-grade primary brain tumors may also be explained by microscopic, infiltrative tumor [25, 26]. In white matter beyond tumor margins defined by contrast-enhanced MRI, and in some cases even beyond surrounding high signal, nests of tumor can be identified in stereotactic biopsy specimens [25]. This is true even in low-grade neoplasms that are grossly well-defined at neurosurgery or on imaging [26].

There are several limitations to our study. First, this is a retrospective investigation and other imaging signs of intracerebral hematoma, such as focal contrast enhancement or multiplicity, may be of similar or greater diagnostic value. A prospective study should be performed to confirm the independent diagnostic value of the VE ratio. Second, this is a highly selected group of patients who were imaged because a referring physician believed MRI during the acute clinical presentation might be of diagnostic benefit. MRI may not be indicated in all patients with acute intracerebral hematoma, since it has only been shown to change the diagnosis in a minority [5]. Third, patient selection may be considered in interpreting our results since some patients succumb to the effects of acute hematoma before radiologic investigation is possible, and therefore our study group probably represents a less gravely ill population.

References

1. Adams R, Victor M, Ropper A (1997) Principles of neurology, 6th edn. McGraw-Hill, New York, pp 834–841

2. Mutlu N, Berry R, Alpers B (1963) Massive cerebral hemorrhage. Clinical and pathological correlation. Arch Neurol 8: 644–661

3. Scott M (1975) Spontaneous intracerebral hematoma caused by cerebral neoplasms. J Neurosurg 42: 338–342

4. Griffiths P, Beveridge C, Gholkar A (1997) Angiography in non-traumatic brain hematoma. Acta Radiol 38: 797–802

5. Dylewski D, Morgenstern L, Demchuk A (2000) Utility of magnetic resonance imaging in acute intracerebral hemorrhage. J Neuroimaging 10: 78–83

6. Bradley W (1993) MR appearance of hemorrhage in the brain. Radiology 189: 15–26

7. Osborn A (1994) Diagnostic neuroradiology. Mosby-Yearbook, St Louis, pp 166–167

8. Nussbaum E, Heros R, Camarata R (1995) Surgical treatment of intracranial arteriovenous malformations with an analysis of cost-effectiveness. Clin Neurosurg 42: 348–369

9. Duffau H, Capelle L, Sichez JP, et al (1997) Early radiologically proven rebleeding from intracranial cavernous angiomas: report of 6 cases and review of the literature. Acta Neurochir (Wien) 139: 914–922

10. Atlas S, Grossman R, Gomori J, et al (1987) Hemorrhagic intracranial malignant neoplasms: spin-echo MR imaging. Radiology 164: 71–77

11. Inzitari D, Giordano G, Ancona A, Pracucci G, Mascalchi M, Amaducci L (1990) Leukoaraiosis, intracerebral hemorrhage, and arterial hypertension. Stroke 21: 1419–1423

12. Chappell P, Steinberg G, Marks M (1992) Clinically documented hemorrhage in cerebral arteriovenous malformations: MR characteristics. Radiology 183: 719–724

13. Greenberg S, Finkelstein D, Schaefer P (1996) Petechial hemorrhages accompanying lobar hemorrhage: detection by gradient-echo MRI. Neurology 46: 1741–1754

14. Offenbacher H, Fazekas F, Schmidt R, Koch M, Fazekas G, Kapeller P (1996) MR of cerebral abnormalities concomitant with primary intracerebral hematomas. AJNR 17: 573–578

15. Tanaka A, Ueno Y, Nakayama Y, Takano K, Takebayashi S (1999) Small chronic hemorrhages and ischemic lesions in association with spontaneous intracerebral hematomas. Stroke 30: 1637–1642

16. Wakai S, Yamakawa K, Manaka S, Takakura K (1982) Spontaneous intracranial hemorrhage caused by brain tumor. Its incidence and clinical significance. Neurosurgery 10: 437–444

17. Zimmerman H (1984) The pathology of primary brain tumors. Semin Roentgenol 19: 129–138

18. Berkman R, Merrill M, Reinhold W, et al (1993) Expression of vascular permeability factor/vascular endothelial growth factor gene in central nervous system neoplasms. J Clin Invest 91: 153–159

19. Strugar J, Criscuolo G, Rothbart D, Harrington W (1995) Vascular endothelial growth/permeability factor expression in human glioma specimens: correlation with vasogenic brain edema and tumor-associated cysts. J Neurosurg 83: 682–689

20. McLone D (1980) Ultrastructure of the vasculature of central nervous system tumors of childhood. Child's Brain 6: 242–254

21. Criscuolo G (1993) The genesis of peritumoral vasogenic brain edema and tumor cysts: a hypothetical role for tumor-derived vascular permeability factor. Yale J Biol Med 66: 277–314

22. Little J, Dial B, Belanger G, Carpenter S (1979) Brain hemorrhage from intracranial tumor. Stroke 10: 283–288

23. Zimmerman R, Bilaniuk L (1980) Computed tomography of acute intratumoral hemorrhage. Radiology 135: 355–359

24. Senger D, Brown L, Claffey K, Dvorak H (1994) Vascular permeability factor, tumor angiogenesis and stroma generation. Invasion Metastasis 14: 385–394

25. Earnest FT, Kelly P, Scheithauer B, et al (1988) Cerebral astrocytomas: histopathologic correlation of MR and CT contrast enhancement with stereotactic biopsy. Radiology 166: 823–827

26. Coakley K, Huston Jr, Scheithauer B, Forbes G, Kelly P (1995) Pilocytic astrocytomas: well-demarcated magnetic resonance appearance despite frequent infiltration histologically. Mayo Clin Proc 70: 747–751